XXI IMEKO World Congress "Measurement in Research and Industry"
August 30 – September 4, 2015, Prague, Czech Republic

FREQUENCY ESTIMATION IN THE MEASUREMENT TIME BELOW ONE PERIOD

Dušan Agrež

University of Ljubljana, Faculty of Electrical Engineering,
Ljubljana, Slovenia, dusan.agrez@fe.uni-lj.si

Abstract – In paper, a frequency domain estimation algorithm for fast measurement of the signal frequency in the measurement time below one period is presented. When the time is shortened below the signal period, the DC coefficient of the discrete Fourier transformation is taken into account. An analysis is made to study the influence of the leakage effect, offset in the measurement channel, and noise when the Rife-Vincent windows class I (the rectangular window, the Hann window, and others with higher order) are used. Simulations changing the bias of the amplitude DC coefficients support the analysis.

Keywords: frequency estimation, DC amplitude coefficients, Rife-Vincent windows class I, uncertainty, bias error.

1. INTRODUCTION

Traditionally, the frequency is estimated by the time between two zero crossings as well as the calculation of the number of cycles [1]. However, this method is relatively sensitive for distorted signals under harmonics and noise pollution. To suppress this drawback, many fast and accurate frequency estimation methods have been developed during recent years [2], [3]. Some are developed based on the analysis of the voltage frequency spectrum. These methods usually estimate the frequency by searching for the maximum in the spectrum by using, e.g., discrete Fourier transform (DFT) [4], and advanced windowed functions and interpolation schemes have been applied to compensate for the effects of leakage caused by incoherent sampling and finite frequency resolution problems [5], respectively. Real measurement procedures are often encountered with noise components (quantization and thermal noise, switch noise etc.) and harmonic distortions. In these cases some averaging and prefiltering algorithms of measurement signals (interpolations of the time samples, integration by the DFT, etc.) are performed. However, all such methods involve a compromise between the accuracy of the frequency measurement and the length of the observation period; accuracy decreases, as the period becomes smaller.

2. FREQUENCY ESTIMATION BELOW ONE PERIOD TIME

In this paper, an algorithm for fast measurement and estimation of frequency is presented. The algorithm uses discrete time values of the input signal. Sampling by frequency $f_s = 1/\Delta t$ of the periodic band limited analog signal $g(t)$ composed of M components (with f_m, A_m, and φ_m as frequency, amplitude, and phase, respectively) can be expressed as $w(n\Delta t)\cdot\sum_{m=0}^{M-1} A_m \sin(2\pi f_m n\Delta t + \varphi_m)$. To estimate parameters of the time-dependent signals containing any periodicity, it is preferable to use a transformation of the signal in the frequency domain. The discrete Fourier transformation of the windowed signal $w(k)\cdot g(k)$ on N sampled points at the spectral line i is given by:

$$G(i) = -\frac{\mathrm{j}}{2}\sum_{m=0}^{M} A_m \left(W(i-\theta_m)\mathrm{e}^{\mathrm{j}\varphi_m} - W(i+\theta_m)\mathrm{e}^{-\mathrm{j}\varphi_m}\right) \quad (1)$$

where $\theta_m = f_m/\Delta f = i_m + \delta_m$ is the component relative frequency related to base frequency resolution $\Delta f = 1/N\Delta t$ and consists of an integer part and the non-coherent sampling displacement term $-0.5 \le \delta_m < 0.5$.

Shortening of the observation time below the fundamental period causes the leakage disturbances of the DFT coefficients. If there are harmonic components in signal, they participate with the short-range leakage contributions to the amplitude DFT coefficients of interest ($i = 0, 1, 2$) (Fig. 1).

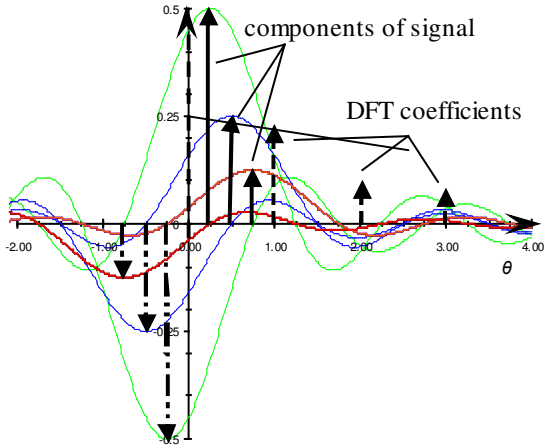

Fig. 1. Influences of harmonic components on the DFT coefficients

The relative position of the fundamental frequency component is between $i=0$ (DC coefficient) and $i=1$, and the first two DFT coefficients are the largest.

If the signal is composed of only one component $m=1$, the DC coefficient can be generally derived from (1):

$$G(0)=-\frac{j}{2}A_m\left[W(-\theta_m)e^{j\varphi_m}-W(\theta_m)e^{-j\varphi_m}\right] \qquad (2)$$

If the function $W(\theta)$ of window used is analytically known, the DFT coefficients can be expressed. For analysis, the well known rectangular and Hann windows are used [6]. For the rectangular window, the following equation is valid, where the amplitude part of Dirichlet kernel is used:

$$\left|W_{\mathrm{R}}(\theta_m)\right|_{N>>1}=\frac{\sin(\pi\theta_m)}{(\pi\theta_m)} \qquad (3)$$

and for the Hann window we have:

$$\left|W_{\mathrm{H}}(\theta_m)\right|_{N>>1}=\frac{\sin(\pi\theta_m)}{2\pi\theta_m(1-\theta_m^2)} \qquad (4)$$

Using window functions for the rectangular window (3) and the Hann window (4) the expression (2) can be rearranged in the following forms:

$$G_{\mathrm{R}}(0)=\frac{A_m}{2}\left[\frac{\sin(-\pi\theta_m)}{(-\pi\theta_m)}e^{-j\left(-a\theta_m-\varphi_m+\frac{\pi}{2}\right)}-\frac{\sin(\pi\theta_m)}{(\pi\theta_m)}e^{-j\left(a\theta_m+\varphi_m+\frac{\pi}{2}\right)}\right]$$

$$G_{\mathrm{R}}(0)=\frac{A_m}{2}\frac{\sin(\pi\theta_m)}{(\pi\theta_m)}\left[e^{-j\left(-a\theta_m-\varphi_m+\frac{\pi}{2}\right)}-e^{-j\left(a\theta_m+\varphi_m+\frac{\pi}{2}\right)}\right] \qquad (5)$$

$$G_{\mathrm{H}}(0)=\frac{A_m}{4}\frac{\sin(\pi\theta_m)}{\pi\theta_m(1-\theta_m^2)}\left[e^{-j\left(-a\theta_m-\varphi_m+\frac{\pi}{2}\right)}-e^{-j\left(a\theta_m+\varphi_m+\frac{\pi}{2}\right)}\right], \qquad (6)$$

where constant a is equal to $a=\pi\cdot(N-1)/N$.

Similar equations for the DFT coefficients at $i=1$ can be written as follows:

$$G(1)=-\frac{j}{2}A_m\left[W(1-\theta_m)e^{j\varphi_m}-W(1+\theta_m)e^{-j\varphi_m}\right]$$

$$G_{\mathrm{R}}(1)=\frac{A_m}{2}\frac{\sin(\pi\theta_m)}{\pi\theta_m}\left[\frac{\theta_m}{1-\theta_m}e^{-j\left(-a\theta_m-\varphi_m+\frac{\pi}{2}\right)}+\frac{\theta_m}{1+\theta_m}e^{-j\left(a\theta_m+\varphi_m+\frac{\pi}{2}\right)}\right] \qquad (7)$$

$$G_{\mathrm{H}}(1)=\frac{A_m}{4}\frac{\sin(\pi\theta_m)}{\pi\theta_m}\left[\frac{1}{(1-\theta_m)(2-\theta_m)}e^{-j\left(-a\theta_m-\varphi_m+\frac{\pi}{2}\right)}-\frac{1}{(1+\theta_m)(2+\theta_m)}e^{-j\left(a\theta_m+\varphi_m+\frac{\pi}{2}\right)}\right] \qquad (8)$$

The complex DFT coefficients (5)-(8) are varying and they are depended upon amplitude, position θ_m, and phase of the searched signal component. The DC component ($i=0$) in the amplitude parts of DFT can be expressed as follows (from (5) and (6)):

$$\left|G_{\mathrm{R}}(0)\right|=\frac{A_m}{2}\frac{\sin(\pi\theta_m)}{(\pi\theta_m)}\left|1-e^{-j2(a\theta_m+\varphi_m)}\right|=\frac{A_m}{2}\frac{\sin(\pi\theta_m)}{(\pi\theta_m)}\left|1-e^{j\Delta\varphi}\right| \qquad (9)$$

$$\left|G_{\mathrm{H}}(0)\right|=\frac{A_m}{4}\frac{\sin(\pi\theta_m)}{\pi\theta_m(1-\theta_m^2)}\left|1-e^{j\Delta\varphi}\right| \qquad (10)$$

The largest values are attained when the exponential part in equations is -1 or the expression $\left|1-e^{j\Delta\varphi}\right|$ is 2. In this case, equations (9) and (10) are composed of only amplitude parts of the used windows (3), (4) (Fig. 2).

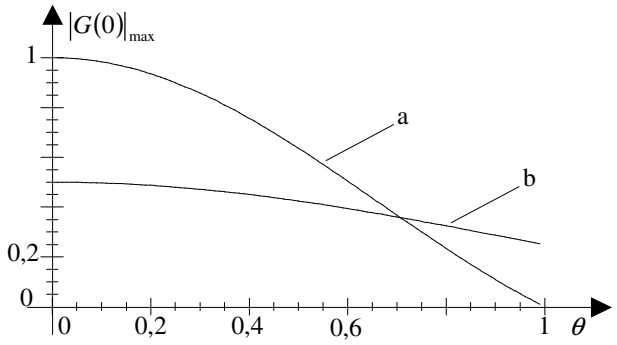

Fig. 2. Maximal values of the short-range leakage influences on the DC coefficient for the rectangular window (a) and for the Hann window (b)

Comparison of the equations (5), (6), (7), and (8) shows, that it is difficult to express the relative frequency without relation to amplitude and phase. This is mathematically pretentious with using only one window ((5) and (7) or (6) and (8)). More success we have, if the DC amplitude coefficients of the rectangular and Hann windowing are used.

$$r_{\mathrm{H,R}}=\frac{\left|G_{\mathrm{H}}(0)\right|}{\left|G_{\mathrm{R}}(0)\right|}=\frac{1}{2(1-\theta_m^2)}\quad\Rightarrow\quad\theta_m=\sqrt{1-\frac{1}{2r_{\mathrm{H,R}}}} \qquad (11)$$

With the quotient $r_{\mathrm{H,R}}$ amplitude, phase, and sinus function in the numerator of (9) and (10) are eliminated, the ratio is constant, and it depends only on the relative frequency (Fig. 3).

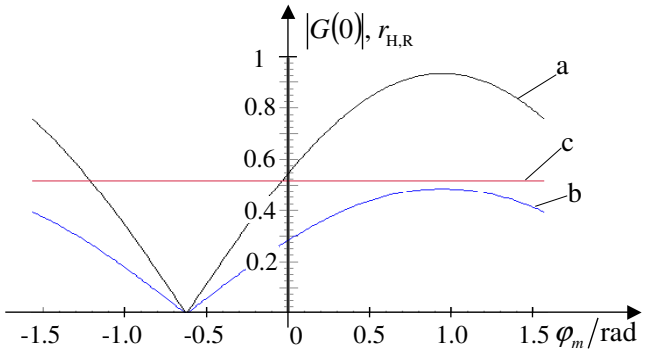

Fig. 3. Amplitude DC coefficients and their quotient $r_{\mathrm{H,R}}$ in relation to phase: a – $\left|G_{\mathrm{R}}(0)\right|$, b – $\left|G_{\mathrm{H}}(0)\right|$, c – quotient $r_{\mathrm{H,R}}$; $\theta_m=0.2$, $A_m=1$, $N=1024$

We can widen this approach of making quotients by DC amplitude DFT coefficients using group of windows defined by D.C. Rife and G.A. Vincent as Rife-Vincent windows class I [7] or windows with the maximal side-lobe decay (MSD) to which the rectangular and the Hann windows belong. Windows RV1 are designed for maximization of the window spectrum side-lobe fall-off:

$$w(n)=\sum_{l=0}^{P}(-1)^l D_{\mathrm{RV1},l}\cdot\cos\left(l\frac{2\pi}{N}\cdot n\right),\quad n=0,1,...,N-1 \quad (12)$$

where $D_{\mathrm{RV1},l}$ are the weighted coefficients of cosines in the window function. The number of the used cosine functions defines window order P. When the order P is zero, the coefficient $D_{1,0}$ is one and equation (12) gives a rectangular shape. If P is one we get the Hann window. Higher values of P expand the window transform main lobe and reduce the spectral leakage. The weighted coefficients can be calculated with $D_{\mathrm{RV1},0}=C_{2P}^{P}/2^{2P}$ and $D_{\mathrm{RV1},l}(P)=C_{2P}^{P-l}/2^{2P-1}$ ($l=1,2,...,P$) using the expression $C_x^y=x!/((x-y)!\,y!)$ [8]. RV1 windows are analytically well-known and the frequency spectrum can be generally expressed as [9],[10]:

$$\begin{aligned}W(\theta)&=\frac{(2P)!}{2^{2P}}\cdot\frac{\sin(\pi\theta)}{\pi\theta}\cdot\frac{1}{\prod_{l=1}^{P}(l^2-\theta^2)}\cdot e^{-j\frac{N-1}{N}\theta}\\&=|W(\theta)|\cdot e^{-j\frac{N-1}{N}\theta}\end{aligned} \quad (13)$$

It can be noticed in (13), that the phase part is not dependent on the window order P and the amplitude part of the RV1 windows which is used in (11) can be generally expressed as follows:

$$|W(\theta)|_{N>>1}=\left|\frac{(2P)!}{2^{2P}}\cdot\frac{\sin(\pi\theta)}{\pi\theta}\cdot\frac{\theta}{\prod_{l=-P}^{P}(l-\theta)}\right| \quad (14)$$

When we use the first two windows in the row of RV1 windows $P=0$ (the rectangular window) and $P=1$ (the Hann window), we get results as in equations (3) and (4):

$$|W_{P=0\leftrightarrow\mathrm{R}}(\theta)|=\left|\frac{(0)!}{2^0}\cdot\frac{\sin(\pi\theta)}{\pi\theta}\cdot\frac{\theta}{(0-\theta)}\right|=\frac{\sin(\pi\theta)}{\pi\theta}$$

$$\begin{aligned}|W(\theta)|_{P=1\leftrightarrow\mathrm{H}}&=\left|\frac{(2)!}{2^2}\cdot\frac{\sin(\pi\theta)}{\pi\theta}\cdot\frac{\theta}{(-1-\theta)(-\theta)(1-\theta)}\right|=\\&=\left|\frac{1}{2}\cdot\frac{\sin(\pi\theta)}{\pi\theta}\cdot\frac{1}{(1-\theta^2)}\right|\end{aligned}$$

$$r_{1,0}=\frac{|G_{P=1\leftrightarrow\mathrm{H}}(0)|}{|G_{P=0\leftrightarrow\mathrm{R}}(0)|}=\frac{1}{2(1-\theta_m^2)}\quad\Rightarrow\quad\theta_m=\sqrt{1-\frac{1}{2r_{1,0}}}$$

We can use this approach with RV1 windows using successive values of orders $P+1$ and P. Quotients of the DC amplitude DFT coefficients can be generally expressed as follows:

$$r_{P+1,P}=\frac{|G_{P+1}(0)|}{|G_P(0)|}=\frac{\left|\frac{(2(P+1))!}{2^{2(P+1)}}\cdot\frac{\sin(\pi\theta)}{\pi\theta}\cdot\frac{\theta}{\prod_{l=-(P+1)}^{(P+1)}(l-\theta)}\right|}{\left|\frac{(2P)!}{2^{2P}}\cdot\frac{\sin(\pi\theta)}{\pi\theta}\cdot\frac{\theta}{\prod_{l=-P}^{P}(l-\theta)}\right|}$$

$$\begin{aligned}r_{P+1,P}&=\left|\frac{(2P+1)(2P+2)}{2^2}\cdot\frac{1}{-(P+1-\theta)(P+1+\theta)}\right|=\\&=\frac{(2P+1)(2P+2)}{4\cdot((P+1)^2-\theta^2)}\end{aligned} \quad (15)$$

and from here the relative frequency can be expressed:

$$\theta_m=\sqrt{(P+1)^2-\frac{(2P+1)(2P+2)}{4\cdot r_{P+1,P}}} \quad (16)$$

Quotients $r_{1,0}$ (11), $r_{2,1}$ (17), and $r_{3,2}$ (18) are phase independent (Fig. 4).

$$r_{2,1}=\frac{|G_2(0)|}{|G_1(0)|}=\frac{(3)(4)}{4\cdot((2)^2-\theta^2)}=\frac{3}{(4-\theta^2)}\quad\Rightarrow\quad\theta_m=\sqrt{4-\frac{3}{r_{2,1}}} \quad (17)$$

$$r_{3,2}=\frac{|G_3(0)|}{|G_2(0)|}=\frac{(5)(6)}{4\cdot((3)^2-\theta^2)}=\frac{15/2}{(9-\theta^2)}\Rightarrow\quad\theta_m=\sqrt{9-\frac{15/2}{r_{3,2}}} \quad (18)$$

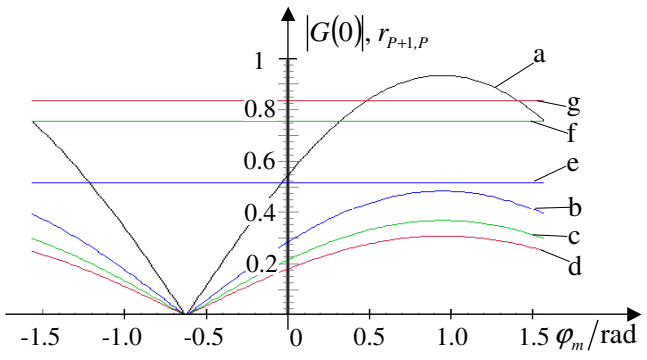

Fig. 4. Amplitude DC coefficients and their quotient $r_{P+1,P}$ in relation to phase: a – $|G_{\mathrm{R}\leftrightarrow P=0}(0)|$, b – $|G_{\mathrm{H}\leftrightarrow P=1}(0)|$, c– $|G_{P=2}(0)|$, d – $|G_{P=3}(0)|$, e – quotient $r_{1,0}$, e – quotient $r_{2,1}$, e – quotient $r_{3,2}$; $\theta_m=0.2$, $A_m=1$, $N=1024$

Values of the DC amplitude DFT coefficients decrease with the window order (Fig. 4: curves a, b, c, and d) but quotients increase (Fig. 4: curves e, f, and g) since increasing the order of RV1 windows widen the window main lobe and the relative distance from window origin – position of the component – decreases.

From the values of the quotients, which are phase and amplitude independent, we can express the relative frequency by (16). Fig. 5 shows error behaviors of the frequency estimations $E(\theta)=\theta_{\mathrm{est}}-\theta_{\mathrm{true}}$ in dependence to the relative frequency in the interval $0.01\le\theta\le1$.

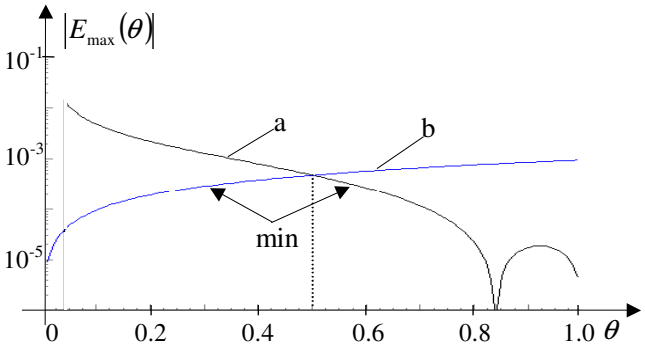

Fig. 5. Absolute maximum values of errors of the frequency estimation in relation to the relative frequency; a – using quotient $r_{1,0}$ and (11), b – using quotient $r_{2,1}$ and (17) or using quotient $r_{3,2}$ and (18); $\theta_m = 0.2$, $A_m = 1$, $N = 1024$

The error behaviors change when using quotient $r_{1,0}$ and estimation (11) (Fig. 5: curve a) and using quotient $r_{2,1}$ and estimation (17) or quotient $r_{3,2}$ and estimation (18) (Fig. 5: curve b). Increasing the window orders in (15) and (16) doesn't change the error behavior of estimations. When the relative frequency is bellow $\theta \le 0.5$ it is better to use quotient $r_{2,1}$ and estimation (17) since this estimation gives lower errors than using quotient $r_{1,0}$ and (11), and above $\theta > 0.5$ it is an opposite situation.

Frequency estimation errors depend on the number of points in the measurement interval. The shapes of errors remain the same but their values drop (Fig. 6). With the measurement interval of half of the signal period ($\theta_m = 0.5$) the estimation errors drop below 10^{-3} if we have more than 1000 points in the measurement interval.

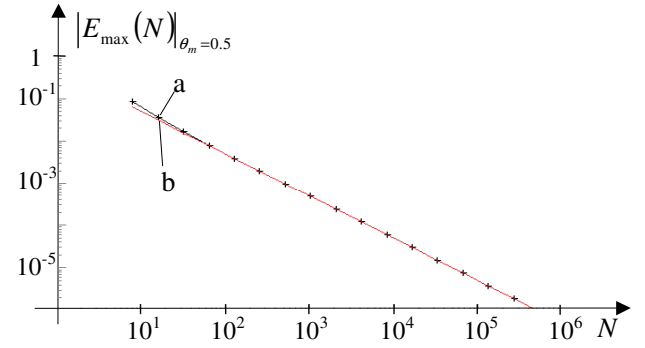

Fig. 6. Absolute maximum values of errors of the frequency estimation in relation to the number of points in the measurement interval; a – using quotient $r_{1,0}$ and (11), b – using quotient $r_{2,1}$ and (17); $\theta_m = 0.5$, $A_m = 1$

UNCERTAINTY OF ESTIMATION

The combined standard uncertainty [10] of the frequency estimation with equation $\theta_m = \sqrt{a_1 - a_2 \cdot |G_P(0)|/|G_{P+1}(0)|}$, where constants $a_1 = (P+1)^2$ and $a_2 = (2P+1)(2P+2)/4$ depend only on the window order, can be expressed by:

$$u_C(\theta_m) = \sqrt{[c_1 \cdot u(|G_P(0)|)]^2 + [c_2 \cdot u(|G_{P+1}(0)|)]^2} \tag{19}$$

where c_1 and c_2 are the sensitivity coefficients:

$$|c_1| = \left|\frac{\partial \theta_m}{\partial |G_P(0)|}\right| = \frac{a_2}{2\sqrt{a_1 - a_2 \cdot |G_P(0)|/|G_{P+1}(0)|}} \cdot \left(\frac{1}{|G_{P+1}(0)|}\right)$$

$$|c_2| = \left|\frac{\partial \theta_m}{\partial |G_{P+1}(0)|}\right| = \frac{a_2}{2\sqrt{a_1 - a_2 \cdot |G_P(0)|/|G_{P+1}(0)|}} \cdot \left(\frac{|G_P(0)|}{|G_{P+1}(0)|^2}\right) \tag{20}$$

Sensitivity coefficients mainly depend upon the phase (Fig. 7) or better position of the measurement window on the signal. The worse position of measurement window is that around the signal zero crossing where DC coefficients are zero (Fig. 4: around $\varphi \approx -0.6$ rad for $\theta_m = 0.2$) and we have very high sensitivity for any DC bias error in the signal. The best position of the window is that on the signal top or bottom where the minimum values of the sensitivity coefficients are attain (Figs. 7 and 8: $c_{1,\min}(\varphi)$, $c_{2,\min}(\varphi)$). To achieve this optimal position one needs to move the measurement window along time axis a little more than quarter of the signal period in the worse.

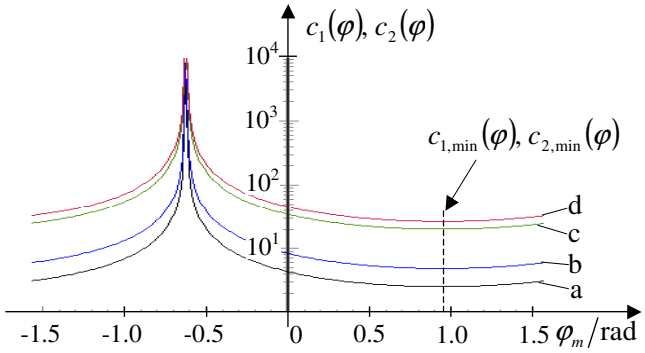

Fig. 7. Sensitivity coefficients in relation to phase: a – $|c_1|_{P=0}$, b – $|c_2|_{P=0}$, c– $|c_1|_{P=1}$, d – $|c_2|_{P=1}$; $\theta_m = 0.2$, $A_m = 1$, $N = 1024$

Optimal positions of the measurement window for minimal errors change with the relative frequency (Fig. 9).

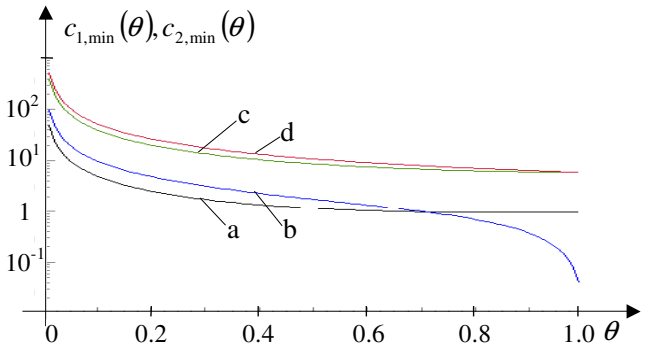

Fig. 8. Minimum values of the sensitivity coefficients in relation to the relative frequency: a – $|c_1|_{P=0}$, b – $|c_2|_{P=0}$, c– $|c_1|_{P=1}$, d – $|c_2|_{P=1}$; $A_m = 1$, $N = 1024$

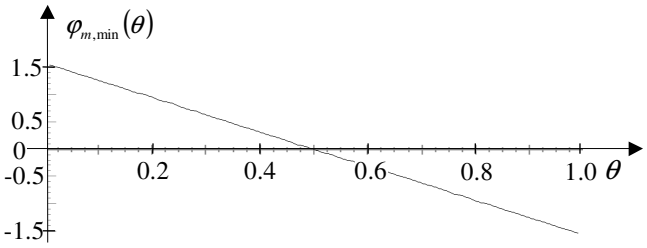

Fig. 9. Phase of the minimum estimation error in relation to the relative frequency; $A_m = 1$, $N = 1024$

Uncertainties of the DC coefficients $u(|G_P(0)|)$ and $u(|G_{P+1}(0)|)$ are adversely affected by offset contribution of the measurement channel, noise and harmonic components in the sampled signal. In analysis, phases of the minimum estimation errors from Fig. 9 are used.

Adding offset to the signal $\Delta_{P,\text{off}}$ (21), as it is a normal situation in the real measurement channel, the quotient is mainly distorted around the worse position of measurement window - around the signal zero crossing (Figs. 10 and 11).

$$r_{P+1,P} = \frac{|G_{P+1}(0)| + \Delta_{P+1,\text{off}}}{|G_P(0)| + \Delta_{P,\text{off}}} = \\ = \frac{|G_{P+1}(0)|}{|G_P(0)|} \cdot \frac{1 + \Delta_{P+1,\text{off}} / |G_{P+1}(0)|}{1 + \Delta_{P,\text{off}} / |G_P(0)|} \approx \frac{|G_{P+1}(0)|}{|G_P(0)|} \quad (21)$$

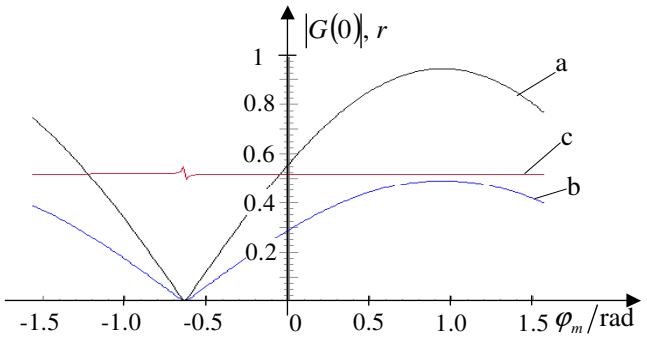

Fig. 10. Amplitude DC coefficients and their quotient $r_{1,0}$ in relation to phase: a – $|G_R(0)|$, b – $|G_H(0)|$, c – quotient $r_{1,0}$; $\theta_m = 0.2$, $A_m = 1$, $N = 1024$, $A_{\text{off}} = 10^{-2}$

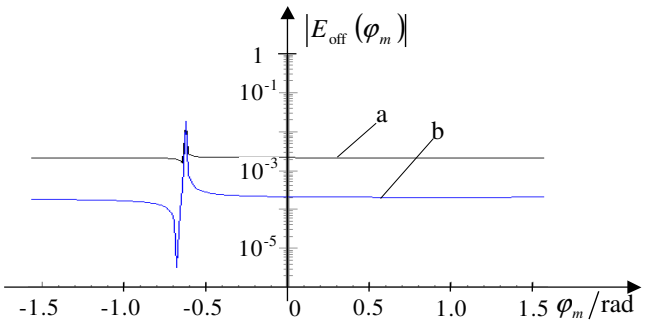

Fig. 11. Absolute values of errors of the frequency estimation in relation to phase; a – $\theta_m = \sqrt{1 - 1/2r_{1,0}}$, b – $\theta_m = \sqrt{4 - 3/r_{2,1}}$; $N = 1024$, $\theta_m = 0.2$, $A_{\text{off}} = 10^{-3}$

Using phase values which give minimal errors (Fig. 9) in estimation by quotient $r_{2,1}$ and (17) gives much better results than by $r_{1,0}$ and (11) below relative frequency $\theta \le 0.5$ (Figs. 12 and 13). Adding offset of one hundred of the signal amplitude, what could be the upper border of the real measurement setup, the frequency estimation error is below 10^{-3} if the relative frequency is under $\theta \le 0.2$ (Fig. 12).

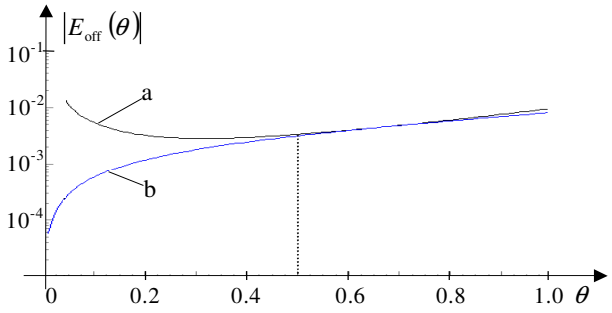

Fig. 12. Absolute values of errors of the frequency estimation in relation to the relative frequency; a – using quotient $r_{1,0}$ and (11), b – using quotient $r_{2,1}$ and (17); $A_m = 1$, $A_{\text{off}} = 10^{-2}$, $N = 1024$

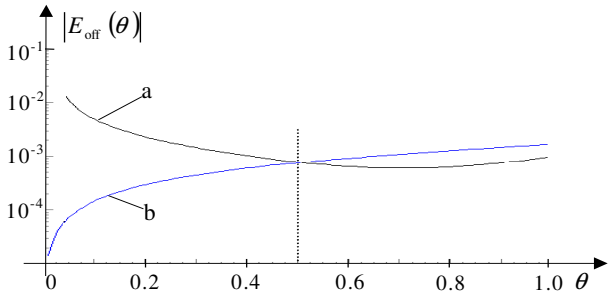

Fig. 13. Absolute values of errors of the frequency estimation in relation to the relative frequency; a – using quotient $r_{1,0}$ and (11), b – using quotient $r_{2,1}$ and (17); $A_m = 1$, $A_{\text{off}} = 10^{-3}$, $N = 1024$

The noise influence on the amplitude coefficient at $i = 0$ is in the first approximation modeled with Gaussian noise $\sigma_{\text{DFT}} = \sigma_t \cdot \sqrt{ENBW} / \sqrt{N}$ [6]. Distortions of the DFT coefficients and the noise uncertainty are decreased with the square root of a number of points N. Standard deviations of estimations increase using higher order P of RV1 windows in estimations (Fig.14) due to higher values of $ENBW \ge 1$.

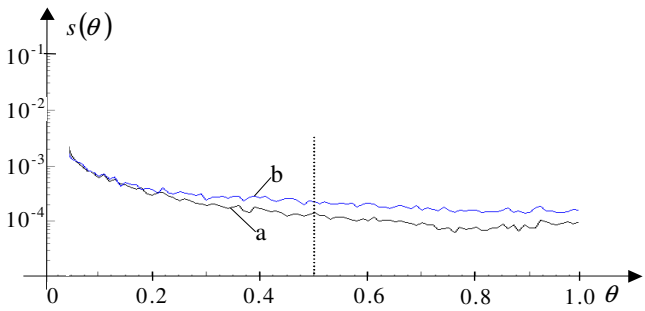

Fig. 14. Standard deviation of the frequency estimation in relation to the relative frequency with added noise $A_{\text{noise}} = 10^{-2}$; a – using quotient $r_{1,0}$ and (11), b – using quotient $r_{2,1}$ and (17); $A_m = 1$, $N = 1024$, 100 trials

Harmonic components in power systems cause additional distortions in measurement procedures. The influences depend on positions of components and they attain the maximal values as it is shown in Fig. 1. If the signal has the second harmonic component as the most disturbing component due to it's closeness to the fundamental component the estimation errors behave like if the offset is presented in the signal (Fig. 15 $\leftrightarrow$ Fig. 10).

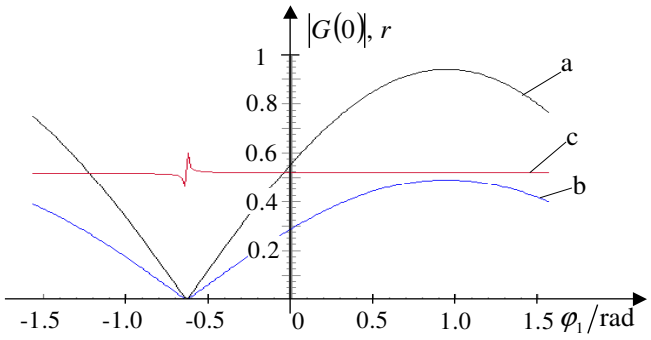

Fig. 15. Amplitude DC coefficients and their quotient $r_{1,0}$ in relation to phase: a – $|G_R(0)|$, b – $|G_H(0)|$, c – quotient $r_{1,0}$; $\theta = 0.2$, $N = 1024$, $A_1 = 1$, $A_2 = 0.01$, $\varphi_2 = 0$

The frequency estimation errors are lower using quotient $r_{1,0}$ and (11) due to narrower window main lobes of the rectangular and the Hann windows (Figs. 16 and 17) but they remain under $3 \cdot 10^{-2}$ if the signal has the second harmonic on the level of one tenth of the fundamental component (Fig. 17: $A_2 = A_1/10$).

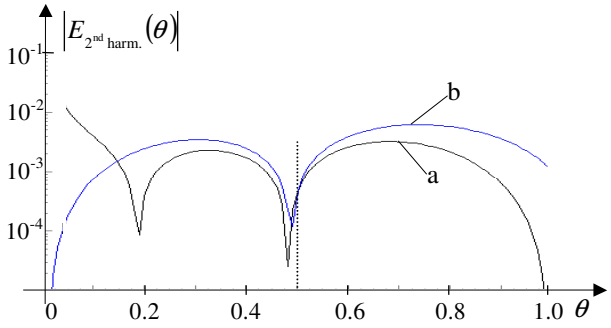

Fig. 16. Absolute values of errors of the frequency estimation in relation to the relative frequency; a – using quotient $r_{1,0}$ and (11), b – using quotient $r_{2,1}$ and (17); $A_m = 1$, $A_2 = 0.01$, $N = 1024$

Harmonic components in the signal disturb the estimation of relative frequency of the fundamental component but if they are under certain level ($THD \approx 1\%$) the errors drop on the level of 10^{-3} (Fig. 16), what could be accepted in many applications of fast tracking and measurement of the frequency.

Elimination of harmonic component can be realized also with filtering [3], but the measurement time increases.

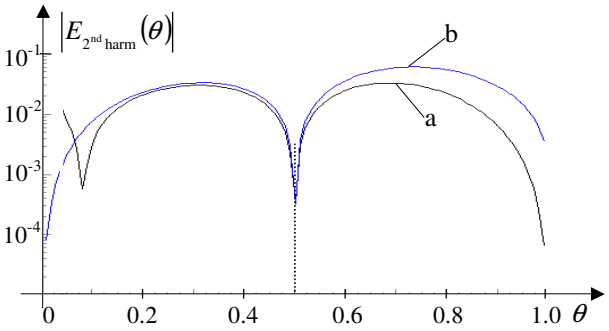

Fig. 17. Absolute values of errors of the frequency estimation in relation to the relative frequency; a – using quotient $r_{1,0}$ and (11), b – using quotient $r_{2,1}$ and (17); $A_m = 1$, $A_2 = 0.1$, $N = 1024$

4. CONCLUSIONS

In the proposed paper, frequency is estimated from the amplitude DFT coefficients. When the time is shortened below the signal period, the DC coefficients using a couple of the RV1 windows with successive order P and P+1 are taken into account. Estimation errors mainly depend on the bias caused either by channel offset or harmonics' influence and can be reduced on the error level of 10^{-3} if the measurement window is positioned at the signal peaks. The complete estimation time is about a half of the period.

REFERENCES

[1] V. Backmutsky, V. Zmudikov, A. Agizim, and G. Vaisman, "A new DSP method for precise dynamic measurement of the actual power-line frequency and its data acquisition applications," Measurement, vol. 18, no. 3, pp. 169-176, 1996.

[2] P. Regulski and V. Terzija, "Estimation of frequency and fundamental power components using an unscented Kalman filter," *IEEE Trans. Instrum. Meas.*, vol. 61, no. 4, pp. 952-962, Apr. 2012.

[3] M. D. Kušljević, "On LS-based power frequency estimation algorithms," *IEEE Trans. Instrum. Meas.*, vol. 62, no. 7, pp. 2020-2028, July 2013.

[4] J. Štremfelj and D. Agrež, "'Nonparametric estimation of power quantities in the frequency domain using Rife-Vincent windows," *IEEE Trans. Instrum. Meas.*, vol. 62, no. 8, pp. 2171-2184, Aug. 2013.

[5] T. Radil, P. M. Ramos, and A. C. Serra, "New spectrum leakage correction algorithm for frequency estimation of power system signals," *IEEE Trans. Instrum. Meas.*, vol. 58, no. 5, pp. 1670–1679, May 2009.

[6] F. J. Harris, "On the Use of Windows for Harmonic Analysis with the Discrete Fourier Transform," *Proceedings of the IEEE*, vol. 66, no. 1, pp. 51-83, January 1978.

[7] D. C. Rife, G. A. Vincent, Use of the discrete Fourier transform in measurement of frequencies and levels of tones, Bell Syst. Tech. J. 49 (1976) 197-228.

[8] D. Belega, D. Dallet, Multifrequency signal analysis by interpolated DFT method with maximum sidelobe decay windows, Measurement 42 (2009) 420-426.

[9] H.H. Albrecht, A family of cosine-sum windows for high-resolution measurements, in: Proceedings of ICASSP'01 (2001) 3081-3084.

[10] JCGM, Evaluation of measurement data — Guide to the expression of uncertainty in measurement, Sept. 2008.